Carcinogenesis, 2022, **43**, 601–610
https://doi.org/10.1093/carcin/bgac029
Advance access publication 12 March 2022
Original Article

Original Article

Cribriform-type adenocarcinoma of the colorectum: comprehensive molecular analyses of a distinctive histologic subtype of colorectal cancer

Shun Yamada[1,2], Mitsumasa Osakabe[1], Makoto Eizuka[2], Mai Hashimoto[1], Noriyuki Uesugi[1], Naoki Yanagawa[1], Koki Otsuka[3], Hiromu Suzuki[4], Takayuki Matsumoto[2] and Tamotsu Sugai[1,*]

[1]Department of Molecular Diagnostic Pathology, School of Medicine, Iwate Medical University, Yahaba, Japan
[2]Division of Gastroenterology, Department of Internal Medicine, School of Medicine, Iwate Medical University, Yahaba, Japan
[3]Department of Surgery, School of Medicine, Iwate Medical University, Yahaba, Japan and
[4]Department of Molecular Biology, School of Medicine, Sapporo Medical University, Sapporo, Japan

*To whom correspondence should be addressed. Department of Molecular Diagnostic Pathology, School of Medicine, Iwate Medical University, 2-1-1, Idaidori, Yahaba 028-3695, Japan. Tel: +81 19 613 7111; Fax: +81 19 611 8071; Email: tsugai@iwate-med.ac.jp

Abstract

Colorectal adenocarcinoma (CRA) is characterized by marked heterogeneity and may be composed of an admixture of various histologic patterns, including well-formed gland and cribriform types. Although tumors displaying a prominent or predominant cribriform feature are frequently found in CRA, this type may contain specific histologic variants with a characteristic molecular alteration. We investigated the molecular features of 51 primary CRAs with a predominant cribriform histology using array-based analyses [somatic copy number alterations (SCNAs); mRNA expression]. Mutations (*TP53, KRAS, PIK3CA* and *BRAF*) and DNA methylation status were also analyzed. The crypt isolation method was used to obtain isolated tumor glands of each type separately. All patients were classified by their CRA histologic subtype into two groups: well-formed gland and cribriform. Next, we performed cluster analysis to stratify SCNA and mRNA expression patterns between the two subtypes. Two distinctive subgroups were stratified based on patterns of SCNA and mRNA expression and were correlated with each histologic subtype. The cribriform type was characterized by a high frequency of SCNA compared with that of the well-formed gland type and was closely associated with the expression of specific mRNAs. In addition, the frequency of *KRAS* mutation was significantly higher in the cribriform type than in the well-formed gland type. Finally, there was no difference in DNA methylation status between the two subtypes. Overall, these data suggest that the cribriform type provides important insights into colorectal carcinogenesis, suggesting specific potential histologic implications based on the molecular profile.

Graphical Abstract

Molecular characteristics of cribriform-type adenocarcinoma of colorectum.

Abbreviations: CRA, colorectal adenocarcinoma; CRC, colorectal cancer; SCNA, somatic copy number alteration

Introduction

Colorectal cancer (CRC), particularly adenocarcinoma, remains a leading cause of cancer mortality worldwide (1). According to the current World Health Organization (WHO) classification of colorectal adenocarcinoma (CRA), the most common type is differentiated-type adenocarcinoma, termed a conventional adenocarcinoma (2). Although this classification is widely accepted, differentiated-type adenocarcinoma, regardless of being the most common histologic type, is not subdivided in the WHO classification

Received: January 13, 2022; Revised: March 4 2022; Accepted: March 10, 2022

Table 1. Clinicopathological findings of cribriform and well-formed gland-type adenocarcinomas

Variables	Number of cases (%)	Cribriform type (%)	Well-formed gland type (%)	*P*
Total	51 (100.0)	25 (49.0)	26 (51.0)	
Sex				0.0254
Male	26 (51.0)	17 (68.0)	9 (34.6)	
Female	25 (49.0)	8 (32.0)	17 (65.4)	
Age, year, median [range]	72 [42–91]	72 [42–86]	72 [50–91]	0.9323
Location				0.8217
C/A/T/D/S/R	4/5/3/4/16/19	1/3/1/3/8/9	3/2/2/1/8/10	
Size, mm, median [range]	42 [17–80]	40 [17–80]	46 [20–75]	0.9248
Macroscopic type				0.1906
1/2/3/4	6/43/2/0	1/23/1/0	5/20/1/0	
Positive for necrosis	29 (56.9)	15 (60.0)	14 (53.8)	0.7793
Positive for hemorrhage	13 (25.5)	8 (32.0)	5 (19.2)	0.3487
Depth of invasion				0.0337
Muscularis propria/subserosa	16/35	4/21	12/14	
Positive for venous invasion	24 (47.1)	13 (52.0)	11 (42.3)	0.5793
Positive for lymphatic invasion	12 (23.5)	6 (24.0)	6 (23.1)	1.0000
Positive for lymph node metastasis	22 (43.1)	12 (48.0)	10 (38.5)	0.5771
TNM stage				0.1076
I/II/III/IV	15/14/22/0	4/9/12/0	11/5/10/0	

A, ascending colon; C, cecum; D, descending colon; R, rectum; S, sigmoid colon; T, transverse colon.

(2). In contrast, in the Japanese histologic classification, differentiated-type adenocarcinoma includes papillary, well-differentiated and moderately differentiated adenocarcinoma based on the histologic features of the cancer glands (3). Moderately differentiated adenocarcinoma is characterized by a cribriform pattern, whereas well-differentiated or papillary adenocarcinomas, in principle, are defined as tumors with well-formed glands or papillary structures (3). Although intermediate types exist, most gastrointestinal pathologists assign tumors with intermediate features to a variant of either the well-formed type or the cribriform type according to histologic similarity.

In the 2011 WHO classification, cribriform-comedo-type adenocarcinoma was described as a rare specific variant of CRA (4), which is an analog of comedo-type carcinoma of the breast, characterized by central necrosis of the cribriform nest (4). Cribriform-type CRA has specific clinicopathologic features, including a high frequency of venous invasion and organ metastasis (4–6). However, consensus on its clinicopathologic and molecular findings has not been reached, despite its poor prognosis (4–6). Moreover, it was no longer present in the 2019 WHO histologic classification (2). Although CRA with a prominent or predominant cribriform feature is not rare, awareness of this histologic variant is important to establish novel histologic variants in CRA. In addition, identification of specific molecular alterations occurring in cribriform-type cancer cells may provide new insights into colorectal carcinogenesis.

We report the clinicopathologic and molecular differences among CRAs with a predominant cribriform histologic growth pattern, with special emphasis on histopathologic differential diagnosis by comprehensive array-based analysis. In addition, we also describe the *TP53*, *KRAS*, *PIK3CA* and *BRAF* mutational status and discuss the role of molecular carcinogenesis in this type of CRA.

Materials and methods

Patients

Samples (N = 51) were obtained from resected specimens of patients with newly diagnosed, previously untreated, primary CRC at Iwate Medical University between 2017 and 2020. The pathologic diagnosis and clinicopathologic variables were determined according to a combination of the Japanese classification and the WHO classification (2,3). We classified these CRAs into two histologic variants, cribriform and well-formed gland-type adenocarcinomas, based on the area ratio of cribriform type to well-formed gland type (>50% of the tumor) (2). In the present study, no differences in the frequencies of the macroscopic types, necrosis or hemorrhage were found between the subtypes. Necrosis was defined based on extracellular necrosis only (excluding intraluminal necrosis). Male sex and the frequency of subserosal invasion were more strongly associated with the cribriform type than the well-formed gland type. However, no statistically significant differences in the other variables were found between groups. Detailed clinicopathologic findings are listed in Table 1.

This study was approved by the Ethical Research Committee of Iwate Medical University (HG2020-034).

Determination of sample size

This was a retrospective study. The minimum sample size required to identify differences between cribriform-type and well-formed gland-type adenocarcinomas was determined by JMP Pro 16.1 software (SAS, Tokyo, Japan) to be 46 cases. The statistical power was set to 0.8, which is commonly used in medical studies.

Crypt isolation method

Fresh tumor and normal tissues were obtained from resected CRC samples. Normal colonic mucosa was collected from the

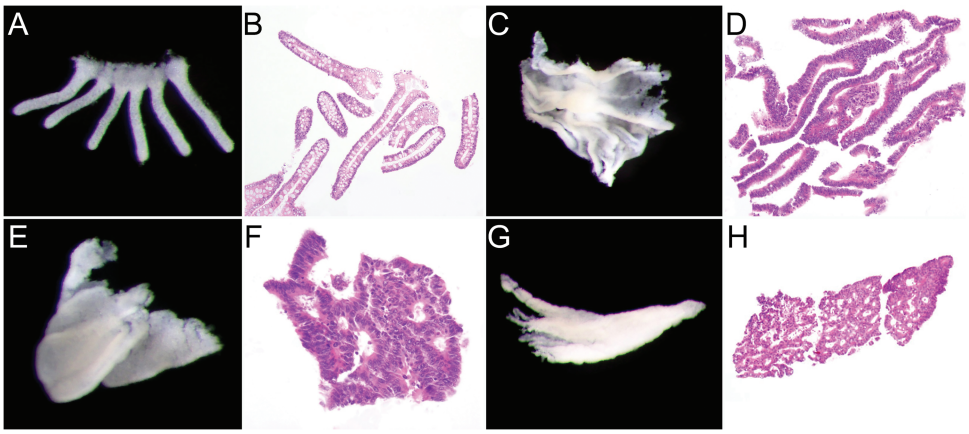

Figure 1. Representative examples of isolated cribriform-type gland and well-formed gland-type carcinoma. (**A**) Normal isolated crypt under a dissecting microscope. (**B**) Histologic features of an isolated crypt. (**C**) Isolated well-formed gland under a dissecting microscope. (**D**) Histologic features of an isolated well-formed gland. (**E**) Isolated cribriform-type gland under a dissecting microscope. (**F**) Histologic features of an isolated cribriform-type gland. (**G**) Isolated cribriform-type gland under a dissecting microscope. (**H**) Histologic features of an isolated cribriform-type gland.

most distal portion of the colon. Cribriform-type and well-formed type glands were collected from cribriform-type and well-formed type adenocarcinomas, respectively, as diagnosed histologically (>50% of the tumor).

Crypt isolation from tumor and normal mucosa was performed as previously reported (7,8). Tumor samples were collected primarily from the central area of tumor ulceration. Briefly, fresh normal mucosa and tumor tissues were minced with a razor and incubated at 37°C for 30 min in calcium- and magnesium-free Hanks' balanced salt solution containing 30 mM ethylenediaminetetraacetic acid. Isolated crypts/glands were immediately fixed in 70% ethanol and stored at 4°C until DNA extraction.

Fixed isolated crypts were observed under a dissecting microscope (SZ60; Olympus, Tokyo, Japan). Based on gland morphology showing differentiated-type adenocarcinoma, cribriform and well-formed glands were obtained separately. The cribriform growth pattern was observed in glands fused together, creating images such as a squid or jellyfish (Figure 1), whereas the well-formed gland type was seen as a tubular structure. Some isolated crypts/glands were processed routinely by histopathologic analysis to confirm their histologic nature. Contamination, such as interstitial cells, was not evident in any sample. Cribriform-type glands showed a glandular cavity structure with back-to-back fused tumor glands with poorly formed glandular spaces lacking intervening stroma. In contrast, well-formed cancer glands had a well-differentiated glandular structure.

DNA extraction

DNA was extracted by standard SDS proteinase K treatment and resuspended in TE buffer [10 mM Tris–HCl, 1 mM ethylenediaminetetraacetic acid (pH 8.0)].

RNA extraction

Total RNA was isolated with RNeasy Mini kits (Qiagen, Valencia, CA) per the manufacturer's instructions. The nucleic acid concentration was determined with a Nanodrop1000 spectrophotometer (Thermo Fisher Scientific; Waltham, MA), and purity was verified on 1.5% agarose denaturing gels.

Analysis of microsatellite instability

Microsatellite instability was determined based on a consensus panel of five reference microsatellite markers (BAT25, BAT26, D2S123, D3S546 and D17S250), as described previously (9). When no marker was altered, tumors were defined as microsatellite stable. When only one marker was altered, tumors were defined as low microsatellite instability. When two or more markers were altered, tumors were defined as high microsatellite instability.

Analysis of mutations

Single-strand conformational polymorphism analysis was used to screen PCR products derived from *TP53* (exons 5–8) and *PIK3CA* (exons 9 and 20) in tumor and normal mucosal DNA samples. PCR conditions, PCR-single-strand conformational polymorphism and *TP53* and *PIK3CA* sequencing were performed as described previously (10). Direct sequencing was performed using fluorescence-labeled dideoxynucleotide triphosphates for automated DNA sequence analysis (Applied Biosystems 373A Sequencer; Applied Biosystems).

Mutations in *KRAS* and *BRAF* were quantified by PCR analysis of bisulfite-modified genomic DNA (EpiTect Bisulfite Kit; Qiagen, Valencia, CA) using pyrosequencing (Pyromark Q24; Qiagen NV), as described previously (11). The primers used are described elsewhere (11).

Analysis of DNA methylation

DNA methylation was quantified at six specific promoters originally described by Yagi *et al.* (12). Briefly, using a panel of three markers (*RUNX3*, *MINT31* and *LOX*), we defined high methylation epigenome tumors as having at least two methylated markers. The remaining tumors were examined using three additional markers (*NEUROG1*, *ELMO1* and *THBD*); intermediate methylation epigenome tumors were defined as having at least two methylated markers. Tumors not classified as high or intermediate methylation epigenome were designated as low methylation epigenome tumors (13). Methylation of *miR-34b* and cyclin-dependent kinase inhibitor 2A was also analyzed, with a cutoff value of 30% of tumor cells, as previously reported (10,11).

SNP array analysis

We examined somatic copy number alterations (SCNAs) using the Cytoscan HD (Thermo Fisher Scientific) platform, which contains more than 1.9 million non-polymorphic markers and over 740 000 single nucleotide polymorphism (SNP) markers, with an average intragenic marker spacing of 880 bps and intergenic marker spacing of 1737 bps. These platforms are composed of microarrays containing non-polymorphic probes for copy number variations from coding and non-coding regions of the human genome as well as polymorphic SNP probes. All procedures were performed according to the manufacturer's instructions. Slides were analyzed with a GeneChip® Scanner 3000 7G (Thermo Fisher Scientific) and Chromosome Analysis Suite (ChAS) Software (Thermo Fisher Scientific).

Classification of SCNAs

We classified SCNA patterns into three subtypes: gain, loss of heterozygosity (LOH) and copy neutral LOH (CN-LOH). LOH was considered a gross chromosomal change resulting in loss of the entire gene and surrounding region; gain was defined as a gross chromosomal change caused by a gain of the entire gene and surrounding region. CN-LOH was defined as LOH without a copy number change (CN = 2). Detailed classification criteria are described elsewhere (13).

Clariom S Human Array and gene expression analysis

For each array experiment, 500 ng of total RNA was used for labeling with the Clariom S Human Array (Thermo Fisher Scientific), which contains 21 453 mRNAs. Probe labeling, chip hybridization and scanning were performed according to the manufacturer's instructions. A Probe Set (gene-exon) was considered expressed if ≥50% of the samples were detected above background (DABG) values below the DABG threshold (DABG < 0.05). Array data were generated with Transcriptome Analysis Console (TAC version 4.0.1.36) and analyzed with the Thermo Fisher Scientific® Chromosome Analysis Suite v.4.1 (ChAS) (Thermo Fisher Scientific).

Hierarchical analysis of SCNAs and mRNA expression

We conducted hierarchical cluster analysis to group samples according to SCNA and mRNA expression patterns. This approach maximized homogeneity and assured the greatest differences between groups. This was achieved with open-access clustering software (Cluster 3.0 software; bonsai.hgc.jp/~mdehoon/software/cluster/software.htm). The clustering algorithm was set to centroid linkage clustering, the standard method used in biological studies.

Statistical analysis

Differences among groups in clinicopathologic variables were analyzed with Fisher's exact test with statistical software (JMP Pro 16.1 software package for Windows; SAS, Tokyo, Japan). Differences in age and tumor size distributions were evaluated with Mann–Whitney's *U* test in JMP Pro 16.1.

Differences in SCNA number, including gain, LOH and CN-LOH were evaluated with Mann–Whitney's *U* test in JMP Pro16.1 (SAS, Tokyo, Japan). Differences in SCNAs between isolated cribriform-type and well-formed gland-type adenocarcinomas were analyzed with Fisher's exact test. A *P* value <0.05 was considered significant. *P* values were adjusted with the Benjamini–Hochberg false discovery rate (FDR) for multiple comparisons.

Differences in mRNA expression levels between cribriform-type and well-formed gland-type adenocarcinomas for isolated cancer and normal glands were analyzed with the interaction analysis methods of Transcriptome Analysis Console 4.0.2 (Thermo Fisher Scientific, MA) (FDR-*P* value <0.05 and Δ Fold change ≥ absolute value 2).

Results

Microsatellite analysis of CRAs

All tumors were classified as microsatellite stable per criteria previously reported (9).

Mutation analyses of TP53, KRAS, PIK3CA and BRAF

TP53 mutations were found in 56.0% (14/25) and 38.5% (10/26) of cribriform and well-formed gland-type adenocarcinomas, respectively. *PIK3CA* mutations were seen in 2 of 25 (8.0%) cribriform-type adenocarcinomas and 4 of 26 (15.4%) well-formed gland-type adenocarcinomas. These differences were not statistically significant. In contrast, mutations in *KRAS* were statistically significantly more common in cribriform-type versus well-formed gland-type adenocarcinomas [48.0% (12/25) versus 19.2% (5/26), respectively]. Transitions were most common (12 cases, 23.5%) in both types. No *BRAF* mutation was detected in either type. Detailed data regarding these mutations are summarized in Table 2.

DNA methylation status

There was no significant difference in the frequency of DNA methylation between cribriform and well-formed gland-type adenocarcinomas. Both types showed a high frequency of low methylation epigenome [cribriform: 19/26 (76.0%); well-formed gland: 16/26 (61.5%)] (Table 2). The frequency of *miR-34b* methylation was 72% (14/25 cribriform-type adenocarcinoma) and 73.1% (19/26 well-formed gland-type adenocarcinoma). Methylation of *cyclin-dependent kinase inhibitor 2A* was low (2/25, 8.0% in cribriform type; 3/26, 11.5% in well-formed gland type; not significant).

Hierarchical analysis of SCNAs in cribriform and well-formed gland-type adenocarcinomas

SCNA patterns were segregated into two subgroups (Figure 2). The frequency of cribriform-type adenocarcinoma was statistically significantly higher in subgroup 1 versus 2 ($P = 0.0002$; Supplementary Table 1, available at *Carcinogenesis* Online).

SCNAs in each subgroup

The median total number of chromosomal aberrations per patient was 404, with a median of 273 gains (range: 73–632), 66 LOHs (range: 0–195) and 16 CN-LOHs (range: 3–158) in subgroup 1. In subgroup 2, the median total number of chromosomal aberrations per patient was 231.5, with a median of 76 gains (range: 2–230), 89 LOHs (range: 0–397) and 25.5 CN-LOHs (range: 3–140). There were significant differences between subgroups in total numbers of SCNAs and median numbers of CN gains (Figure 3A, panels *a* and *d*; $P < 0.001$ for both). No significant differences were found between subgroups in LOH and CN-LOH (Figure 3A, panels *b* and *c*).

Table 2. Molecular analyses of cribriform-type and well-formed gland-type adenocarcinomas

Genes and methylation status	Cribriform type (%)	Well-formed gland type (%)	*P*
Total	25 (100.0)	26 (100.0)	
TP53 mutation positive	14 (56.0)	10 (38.5)	0.2668
Exon 5	4 (16.0)	3 (11.5)	0.7030
Exon 6	2 (8.0)	1 (4.0)	0.6098
Exon 7	4 (16.0)	3 (11.5)	0.7030
Exon 8	4 (16.0)	3 (11.5)	0.7030
PIK3CA mutation positive	2 (8.0)	4 (15.4)	0.6680
Exon 9	0 (0.0)	4 (15.4)	0.1104
Transition	0 (0.0)	3 (11.5)	
Transversion	0 (0.0)	1 (3.9)	
Exon 20	2 (8.0)	0 (0.0)	0.2353
Transition	1 (4.0)	0 (0.0)	
Transversion	1 (4.0)	0 (0.0)	
KRAS mutation positive	12 (48.0)	5 (19.2)	0.0399
Transition	8 (32.0)	4 (15.4)	0.1994
Transversion	4 (16.0)	1 (3.8)	0.1906
DNA methylation status			
High methylation epigenotype	0 (0.0)	1 (3.9)	1.0000
Intermediate methylation epigenotype	6 (24.0)	9 (34.6)	0.5414
Low methylation epigenotype	19 (76.0)	16 (61.5)	0.3678
Methylation of *miR-34b*	18 (72.0)	19 (73.1)	1.0000
Methylation of *CDKN2A*	2 (8.0)	3 (11.5)	1.0000

CDKN2A, *cyclin-dependent kinase inhibitor 2A*.

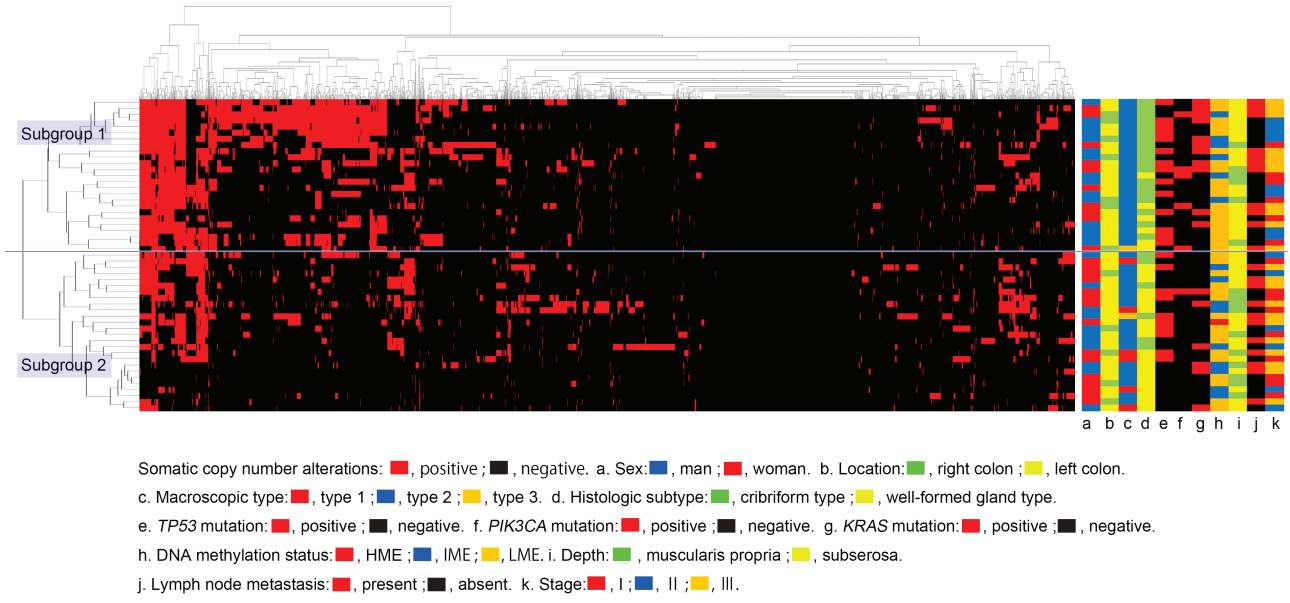

Figure 2. Hierarchical cluster analysis based on SCNA patterns in cribriform-type and well-formed gland-type adenocarcinomas.

Differences in SCNAs between subgroups

The top 5 significant differences in gains between subgroups were found at 6p24.3, 6p24.2, 6p24.1, 6p23 and 6p22.3 (subgroup 1 > 2; Supplementary Table 2, available at *Carcinogenesis* Online). No significant differences in LOH or CN-LOH were observed between subgroups. Detailed data are summarized in Supplementary Table 3 (available at *Carcinogenesis* Online). An ideogram of each lesion is depicted in Supplementary Figure 1 (available at *Carcinogenesis* Online).

SCNAs in each adenocarcinoma type

The median total number of chromosomal aberrations per patient was 227.5, with a median of 85 gains (range: 2–297), 74 LOHs (range: 0–397) and 21 CN-LOHs (range: 3–100) in the well-formed gland type. In cribriform-type

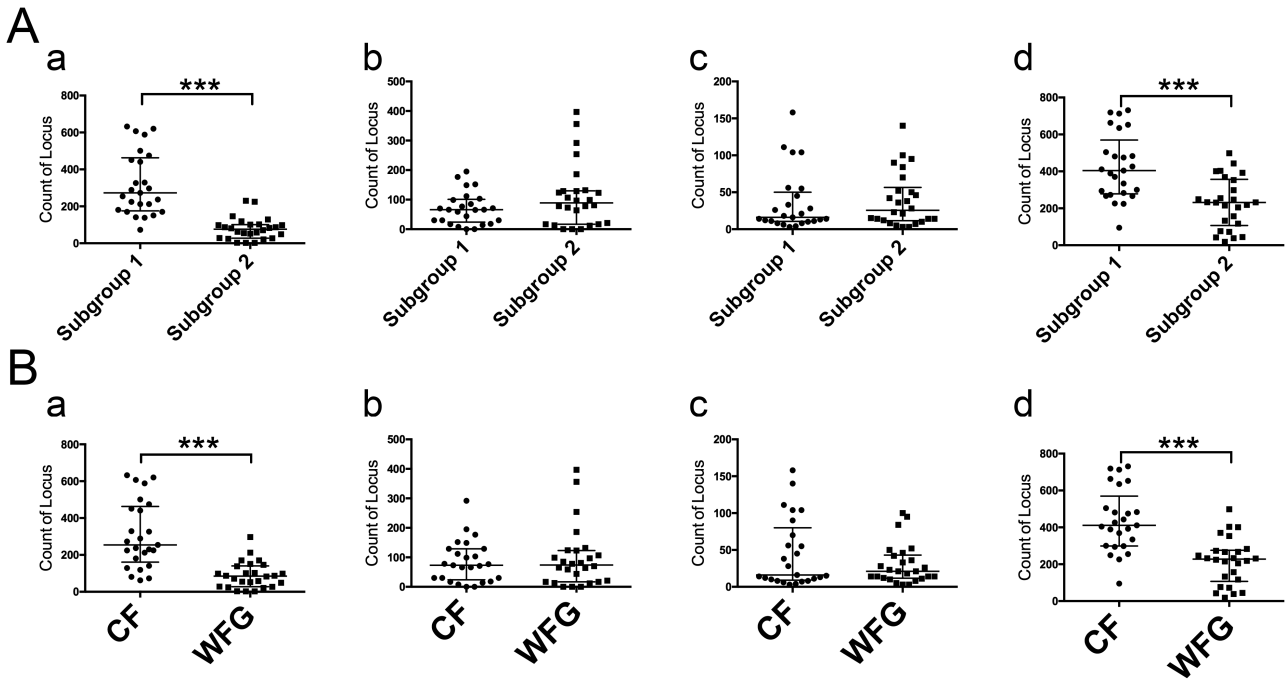

Figure 3. (**A**) Comparison of the total number of SCNAs and the numbers of SCNA gains, SCNA LOHs and SCNA CN-LOHs in 51 CRAs categorized based on SCNAs. (**a**) Comparison of the total number of gains of SCNAs in the two subgroups. (**b**) Comparison of the total number of LOHs in the two subgroups. (**c**) Comparison of the total number of CN-LOHs in the two subgroups. (**d**) Comparison of the total number of overall SCNAs in the two subgroups. (**B**) Comparison of the total number of SCNAs, SCNA gains, SCNA LOHs and SCNA CN-LOHs in 51 CRAs categorized based on SCNAs. (**a**) Comparison of the total number of gains of SCNAs in the CF and WFG types. (**b**) Comparison of the total number of LOHs of SCNAs in the CF and WFG types. (**c**) Comparison of the total number of CN-LOH of SCNAs in the CF and WFG types. (**d**) Comparison of the total number of overall SCNAs in the CF and WFG types. ***$P < 0.001$. CF, cribriform type; WFG, well-formed gland type.

adenocarcinoma, the median total number of chromosomal aberrations per patient was 411, with a median of 254 gains (range: 62–632), 73 LOHs (range: 0–292) and 16 CN-LOHs (range: 3–158). There were significant differences between types in total numbers of SCNAs and median numbers of CN gains (Figure 3B, panels *a* and *d*; $P < 0.001$ for both). No significant differences were found in LOH or CN-LOH between the types (Figure 3B, panels *b* and *c*). In addition, we examined the associations of the SCNA pattern with p-stage, i.e. stage I/II (without metastasis) and stage III/IV (with metastasis). The total number of SCNAs and median number of CN gains were significantly higher in the crbriform type than well-formed gland type in not only stage I/II but also stage III/IV patients (Supplementary Figures 2 and 3, available at *Carcinogenesis* Online). However, no significant difference in the LOH or CN-LOH status was observed between the subtypes (Supplementary Figures 2 and 3, available at *Carcinogenesis* Online).

Regions of gain, LOH and CN-LOH detected in more than 30% of cases are summarized in Supplementary Table 4 (available at *Carcinogenesis* Online).

Differences in SCNAs between adenocarcinoma types

The top 5 regions of gain that differed significantly between cribriform and well-formed gland-type adenocarcinomas were 2p16.3, 2p16.2, 2p16.1, 2p15 and 2p14; no differential regions of LOH or CN-LOH were observed between the two subtypes (Supplementary Table 5, available at *Carcinogenesis* Online). Detailed data are depicted in Supplementary Table 6 (available at *Carcinogenesis* Online). An ideogram of each lesion is depicted in Supplementary Figure 4 (available at *Carcinogenesis* Online).

Associations between the KRAS mutation status and SCNA frequencies in the cribriform and well-formed gland types

We examined the associations between the *KRAS* mutation status and SCNA patterns in both the cribriform type and well-formed gland type. In both subtypes, there was no significant difference in the total number of SCNAs, including gains, LOH and CN-LOH, according to the presence of *KRAS* mutations (Supplementary Figures 5 and 6, available at *Carcinogenesis* Online). However, there was a significant difference in the total number of SCNAs between the types (Supplementary Figures 5 and 6, available at *Carcinogenesis* Online).

Transcriptome analysis of isolated cancer glands

We compared differentially expressed mRNAs of isolated cribriform-type adenocarcinoma with those of isolated well-formed gland-type adenocarcinoma using criteria of FDR-*P* value <0.05 and Δ Fold change ≥ absolute value 2. We identified 180 differentially expressed mRNAs (178 upregulated and 2 downregulated) in cribriform-type samples (Volcano plot; Supplementary Figure 7, available at *Carcinogenesis* Online). Detailed data are shown in Supplementary Table 7 (available at *Carcinogenesis* Online). Cluster analysis identified two distinct subgroups based on mRNA expression pattern (Figure 4). Male, sex and frequency of subserosal invasion were significantly higher in subgroup 1 versus 2, and cribriform-type adenocarcinoma was assigned to subgroup 1 (Supplementary Table 8, available at *Carcinogenesis* Online).

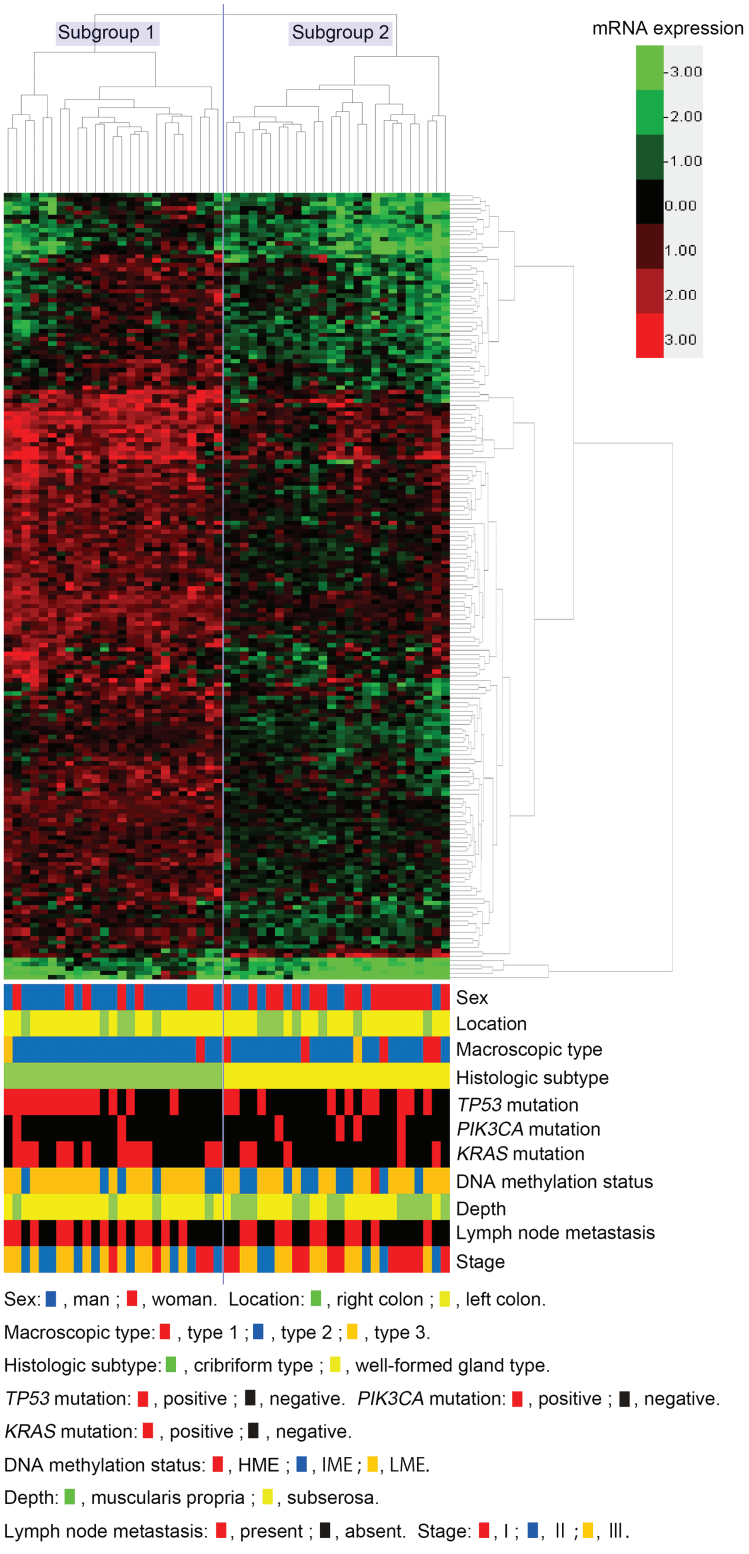

Figure 4. Hierarchical cluster analysis based on the expression pattern of mRNA in the CRAs examined.

Pathway analysis of pooled mRNAs

In a pathway analysis of the 180 dominant mRNAs that characterize cribriform-type adenocarcinoma using a Wikipathway (Transcriptome Analysis Console 4.0.2; TAC), two pathways, including NAD^+ biosynthetic pathways and serotonin receptor 2 and STAT3 signaling were suggested (Supplementary Figures 8 and 9, available at *Carcinogenesis* Online). Transcripts of PARP4 (poly (ADP-ribose) polymerase family member 4) and SIRT6 (sirtuin) pooled in cribriform-type adenocarcinoma are involved in NAD^+ biosynthetic pathways. In addition, GNAQ [guanine nucleotide binding (G protein), q polypeptide] mRNA, also categorized

as cribriform-type adenocarcinoma, is involved in serotonin receptor 2 and STAT3 signaling.

Discussion

CRAs are characterized by histologic heterogeneity (14); adenocarcinomas with a single pure or predominant histologic pattern are rare. Cribriform architecture is not a distinctive pattern in CRA, and tumors displaying this growth pattern are not included in the WHO classification (2), because data may be insufficient to distinguish it from other subtypes. Because of the histologic characteristics, however, the presence of a predominant or exclusive cribriform growth pattern in a CRA generally increases the diagnostic or prognostic novelty of an adenocarcinoma from another conventional type. However, other types of cancer glands, such as papillary (which may include the well-formed gland type), mucinous and solid types of adenocarcinoma, were not included in the present study, as it aimed to identify pathologic and molecular differences between cribriform and well-formed type glands, as those are considered the major types of differentiated-type adenocarcinoma. Future studies will elucidate differences among other types.

Mutations in *TP53* and *KRAS* are common in CRC (15,16). Mutations in *KRAS* may be affected by various factors, including sex, tumor location, pathogenesis (adenoma–carcinoma sequence versus *de novo* pathway), etiology, villous component and prognosis (17–19). However, histologic differences in *KRAS* mutations are not well understood. We found a statistically significant difference in the frequency of *KRAS* mutations between the two subtypes, which may suggest that *KRAS* mutations depend on cribriform-type adenocarcinoma. In addition, the prognostic role of *KRAS* mutations has been debated. Although a study including metastatic CRCs showed no association between *KRAS* mutations and disease-free survival (DFS), most studies, including those on non-metastatic CRC, concluded that *KRAS* mutations are associated with poor disease-free survival (20). Thus, *KRAS* mutations in cribriform-type adenocarcinoma may be associated with prognosis. In contrast, *TP53* mutations were common in both subtypes analyzed, suggesting that mutations in *TP53* may be independent of histologic type and supporting the role of basic mutations in the development of CRC. Finally, mutations of *BRAF* and *PIK3CA* had a minor role in the development of both types.

A critical challenge in the genome-wide analysis of SCNAs is distinguishing the alterations that drive cancer growth from the numerous, apparently random alterations that accumulate during tumorigenesis (21). Accumulation of SCNAs, which results in somatic genome instability, has been the principle of carcinogenesis; cancer cells stem from a clone that has somatically acquired genetic abnormalities, leading to malignant transformation and further progression (21,22). With advances in array-based technologies, interest in evaluating SCNA burden and identifying a specific altered allele responsible for certain cancer types has been growing to identify targeted genomic changes or to assess tumor biology among histologic subtypes (23,24). In the present study, cribriform-type adenocarcinoma was characterized by the accumulation of numerous SCNAs, especially total SCNAs and gain of SCNA. This finding may suggest that the cribriform type is potentially more aggressive than the well-formed gland type. In addition, the current findings may suggest that cribriform-type adenocarcinoma may represent an independent category in terms of SCNAs.

In the present study, gains at 2p14-16 characterized cribriform-type adenocarcinoma. However, gains at 2p14-16 were reported at a low frequency in CRC (14). In a previous study, although CRC was stratified into three subgroups, one had a high frequency of gain at a wide region of 2p containing a narrow region 2p14-16 (25). Identification of target genes will require both genomic and functional studies (25). For focal events, the copy number profiles of higher resolution analysis can help narrow the list of candidates (26). However, we could not find correlations between the region displaying SCNAs at 2p14-16 with corresponding gene expression, which may suggest that genomic changes derived from cancer cells occur randomly during neoplastic progression, regardless of functional alterations in mRNA expression.

Differences in mRNA expression patterns may affect histologic features. Few studies have investigated differences in the expression of individual mRNAs across histologic types in CRC. We found a significant difference in mRNA expression patterns between cribriform and well-formed gland-type adenocarcinomas. In addition, we showed that two pathways, NAD^+ biosynthetic pathways and serotonin receptor 2 and STAT3 signaling, are closely associated with cribriform-type adenocarcinoma (27,28). However, their role in its development remains unknown. *PARP4* and *SIRT6* are important for NAD^+ biosynthetic pathways, whereas *GNAQ* is involved in serotonin receptor 2 and STAT3 signaling (27,28). Although these genes are thought to play an important role in carcinogenesis, in particular, PARP4 and GNAQ should be noticed in colorectal carcinogenesis (29–35).

PARP proteins are involved in cellular processes, including cell survival and death, transcription, DNA repair, telomere integrity and cell division (29–32). PARP1, in conjunction with β-catenin, c-myc, cyclin D1 and MMP-7, plays an important role in colorectal carcinogenesis (32). In addition, interest in developing PARP inhibitors for cancer therapy is increasing (27,28). A PARP inhibitor may be effective in the treatment of cribriform-type adenocarcinoma, given that PARP4 is upregulated in this type of cancer compared with the PARP4 transcript in well-formed glands. Second, aberrations in genes encoding G-protein family-activating subunits have been increasingly implicated in tumorigenesis. G-protein-activating subunits, such as those encoded by *GNAS*, *GNAQ*, *GNA11* and *GNA12*, bind to G-protein-coupled receptors and play central roles in cellular signal transduction (35). G proteins and G-protein-coupled receptors are ubiquitously expressed and are critical throughout transcription, cell division, motility and secretion (34,35). In the present study, GNAQ was found to be upregulated in cribriform-type adenocarcinoma. In addition, mutation of *RAS*, a member of the G protein family (36), was frequently found in cribriform-type adenocarcinoma, suggesting that upregulated GNAQ might enhance *KRAS* mutation, which activates cell proliferation. Parish *et al.* showed that alterations in G-protein-activating subunits frequently co-occurred with several specific alterations in genes including *KRAS*, Aurora kinase A, Src proto-oncogene, Casitas B-lineage lymphoma and LYN proto-oncogene, Src family tyrosine kinase, which also affect critical oncogenic pathways and play important roles in the carcinogenesis of many cancer types (34). Together with the current findings,

this may imply that such alterations affect the development of cribriform-type adenocarcinoma.

DNA methylation plays an important role in colorectal carcinogenesis (11,15,16). In the present study, although two different panels were used, a comprehensive analysis of DNA methylation was not performed. Thus, no significant difference in DNA methylation between the cribriform type and the well-formed gland type was found. We analyzed individual markers, including miR-34b and *cyclin-dependent kinase inhibitor 2A*, which is closely associated with colorectal carcinogenesis (37,38). Methylation of miR-34b showed a high frequency in both types, but no significant difference between types was found. This finding may indicate that miR-34b methylation is a common alteration in both subtypes. Although DNA methylation is considered a fundamental alteration that occurs during early colorectal tumorigenesis (15,16), such as progression from adenoma to cancer, it may not contribute to the molecular differences between the cribriform and well-formed gland types. In addition, our results suggest that there is no difference in DNA methylation in early colorectal tumorigenesis between the subtypes.

Yagi *et al.* indicated that *KRAS* mutations are correlated with an intermediate level of DNA methylation in CRC (12). In the present study, however, although there was a high frequency of *KRAS* mutations in the cribriform type, compared with the well-formed gland type, the DNA methylation level was low in both the well-formed gland and cribriform types, the latter of which shows a high frequency of *KRAS* mutations. However, the reason for this discrepancy remains unknown, and genome-wide DNA methylation analysis may be required.

This study has some limitations. First, the sample size is small. However, we used crypt isolation to obtain pure tumor crypts, which greatly contributes to the identification of molecular alterations among cribriform and well-formed gland-type adenocarcinomas. Although collection of samples of pure cancer glands may be difficult (10,11), we obtained a sufficient number to achieve statistical power. Second, histologic transition from the well-formed gland-type to cribriform-type adenocarcinomas may be important to identify the molecular characteristics of cribriform-type adenocarcinoma. In the present study, however, this was not examined. The present results show an obvious difference in molecular alterations between adenocarcinoma subtypes, suggesting that cribriform-type adenocarcinoma may be more aggressive. Third, a validation cohort was not examined. However, this study contributes to the identification of molecular alterations of cribriform-type adenocarcinoma. Finally, no significant differences in clinicopathologic findings between cribriform and well-formed gland-type adenocarcinomas were observed due to the small case number. In this regard, prognostic data may be required to distinguish the cribriform type from other differentiated-type adenocarcinomas. We intend to analyze patient outcome data of cribriform-type adenocarcinoma in future studies. To the best of our knowledge, this is the first study to examine molecular alterations of cribriform-type CRA comprehensively.

In conclusion, we described pathologic and molecular alterations of primary CRAs characterized by a distinctive and predominantly cribriform histology. Careful clinicopathologic assessment and molecular studies helped establish the primary colorectal origin of these tumors. Accumulation of SCNAs was associated with cribriform-type adenocarcinoma. In addition, expression of specific mRNAs occurring in cribriform-type adenocarcinoma characterized this subtype. Finally, an activating *KRAS* mutation was observed. The high frequency of SCNA and activating mutation of *KRAS* seems to identify a particular molecular signature or predictive therapeutic response in CRA with cribriform histology. This histologic variant is important in evaluating colorectal carcinogenesis.

Supplementary material

Supplementary data are available at *Carcinogenesis* online.

Acknowledgements

We gratefully acknowledge the technical assistance of members of the Department of Molecular Diagnostic Pathology, Iwate Medical University for their support.

Funding

No funding was received for this study.

Conflict of interest statement

None declared.

Authors' contributions

S. Yamada, the first author, constructed the figures and tables and performed the statistical analyses. M. Osakabe assisted with the statistical analyses. N. Uesugi and N. Yanagawa helped in the pathological interpretation of CRC examined. K. Otsuka and T. Matsumoto provided clinical support during the preparation of the manuscript. H. Suzuki supported the molecular examination. T. Sugai, the corresponding author, contributed to the preparation of the manuscript, including all aspects of the data collection and analysis.

Consent of publication

Not applicable.

Ethical approval and consent to participate

Informed consent was obtained from each patient according to institutional guidelines, and the research protocols were approved by the ethics committee of Iwate Medical University Hospital (approval number HG2020-034).

Human rights statement and informed consent

All procedures were performed in accordance with the ethical standards of the Iwate Medical University and with the Declaration of Helsinki. Substitute for informed consent (approval by the institutional review board of Iwate Medical University) was obtained from all patients included in the study.

Data availability

The datasets used and/or analyzed during the current study are available from the corresponding author on reasonable request.

References

1. Siegel, R.L. et al. (2020) Colorectal cancer statistics, 2020. *CA Cancer J. Clin.*, 70, 145–164.
2. Nagtegaal, I.D. et al. (2019) Colorectal adenocarcinoma. In Nagtegaal, I.D. et al. (eds) *WHO Classification of Tumours of the Digestive System*. International Agency for Research on Cancer Lyon, pp. 177–187.
3. Japanese Society for Cancer of the Colon and Rectum. (2009) *Japanese Classification of Colorectal Carcinoma*. 2nd English edn. Kanehara & Co. Tokyo, pp. 30–63.
4. Taylor, A.S. et al. (2021) Cribriform colon cancer: a morphological growth pattern associated with extramural venous invasion, nodal metastases and microsatellite stability. *J. Clin. Pathol.*, 29, jclinpath-2021-207485.
5. Díaz Del Arco, C. et al. (2019) Colorectal cribriform comedo-type adenocarcinoma: a distinct subtype with poor prognosis? *Acta Gastroenterol. Belg.*, 82, 329–332.
6. Aust, D.E. (2011) WHO classification 2010 for the lower gastrointestinal tract: what is new? *Pathologe*, 32 (suppl. 2), 326–331.
7. Habano, W. et al. (1996) A novel method for gene analysis of colorectal carcinomas using a crypt isolation technique. *Lab. Invest.*, 74, 933–940.
8. Takahashi, H. et al. (2002) Application of the crypt isolation technique to the assessment of genetic alterations of colorectal carcinomas. *Pathol. Int.*, 52, 628–635.
9. Boland, C.R. et al. (1998) A National Cancer Institute Workshop on Microsatellite Instability for cancer detection and familial predisposition: development of international criteria for the determination of microsatellite instability in colorectal cancer. *Cancer Res.*, 58, 5248–5257.
10. Sugai, T. et al. (2000) A unique method for mutation analysis of tumor suppressor genes in colorectal carcinomas using a crypt isolation technique. *Arch. Pathol. Lab. Med.*, 124, 382–386.
11. Sugai, T. et al. (2017) Molecular subtypes of colorectal cancers determined by PCR-based analysis. *Cancer Sci.*, 108, 427–434.
12. Yagi, K. et al. (2012) Intermediate methylation epigenotype and its correlation to KRAS mutation in conventional colorectal adenoma. *Am. J. Pathol.*, 180, 616–625.
13. Tsuyukubo, T. et al. (2020) Comprehensive analysis of somatic copy number alterations in clear cell renal cell carcinoma. *Mol. Carcinog.*, 59, 412–424.
14. Sagaert, X. et al. (2018) Tumor heterogeneity in colorectal cancer: what do we know so far? *Pathobiology*, 85, 72–84.
15. Cancer Genome Atlas Network. (2012) Comprehensive molecular characterization of human colon and rectal cancer. *Nature*, 487, 330–337.
16. Ogino, S. et al. (2008) Molecular classification and correlates in colorectal cancer. *J. Mol. Diagn.*, 10, 13–27.
17. Zauber, P. et al. (2013) KRAS gene mutations are more common in colorectal villous adenomas and in situ carcinomas than in carcinomas. *Int. J. Mol. Epidemiol. Genet.*, 4, 1–10.
18. Sawicki, T. et al. (2021) A review of colorectal cancer in terms of epidemiology, risk factors, development, symptoms and diagnosis. *Cancers (Basel)*, 13, 2025–2047.
19. Yu, J. et al. (2015) Novel recurrently mutated genes and a prognostic mutation signature in colorectal cancer. *Gut*, 64, 636–645.
20. Lee, H.S. et al. (2020) Histology and its prognostic effect on KRAS-mutated colorectal carcinomas in Korea. *Oncol. Lett.*, 20, 655–666.
21. Wang, H. et al. (2016) Somatic gene copy number alterations in colorectal cancer: new quest for cancer drivers and biomarkers. *Oncogene*, 35, 2011–2019.
22. Hastings, P.J. et al. (2009) Mechanisms of change in gene copy number. *Nat. Rev. Genet.*, 10, 551–564.
23. Sugai, T. et al. (2018) Comprehensive molecular analysis based on somatic copy number alterations in intramucosal colorectal neoplasias and early invasive colorectal cancers. *Oncotarget*, 9, 22895–22906.
24. Eizuka, M. et al. (2017) Molecular alterations in colorectal adenomas and intramucosal adenocarcinomas defined by high-density single-nucleotide polymorphism arrays. *J. Gastroenterol.*, 52, 1158–1168.
25. Sugai, T. et al. (2018) Molecular profiling and genome-wide analysis based on somatic copy number alterations in advanced colorectal cancers. *Mol. Carcinog.*, 57, 451–461.
26. Sugai, T. et al. (2021) A genome-wide study of the relationship between chromosomal abnormalities and gene expression in colorectal tumors. *Genes Chromosomes Cancer*, 60, 250–262.
27. Pramono, A.A. et al. (2020) NAD- and NADPH-contributing enzymes as therapeutic targets in cancer: an overview. *Biomolecules*, 10, 358–375.
28. Karmakar, S. et al. (2021) Role of serotonin receptor signaling in cancer cells and anti-tumor immunity. *Theranostics*, 11, 5296–5312.
29. Long, N.P. et al. (2016) Novel biomarker candidates for colorectal cancer metastasis: a meta-analysis of in vitro studies. *Cancer Inform.*, 15 (suppl. 4), 11–17.
30. Michels, J. et al. (2014) Predictive biomarkers for cancer therapy with PARP inhibitors. *Oncogene*, 33, 3894–3907.
31. Mangerich, A. et al. (2011) How to kill tumor cells with inhibitors of poly(ADP-ribosyl)ation. *Int. J. Cancer*, 128, 251–265.
32. Nosho, K. et al. (2006) Overexpression of poly(ADP-ribose) polymerase-1 (PARP-1) in the early stage of colorectal carcinogenesis. *Eur. J. Cancer*, 42, 2374–2381.
33. Dörsam, B. et al. (2018) PARP-1 protects against colorectal tumor induction, but promotes inflammation-driven colorectal tumor progression. *Proc. Natl. Acad. Sci. USA*, 115, 4061–4070.
34. Parish, A.J. et al. (2018) GNAS, GNAQ, and GNA11 alterations in patients with diverse cancers. *Cancer*, 124, 4080–4089.
35. Bockaert, J. et al. (1999) Molecular tinkering of G protein-coupled receptors: an evolutionary success. *EMBO J.*, 18, 1723–1729.
36. Pantsar, T. (2019) The current understanding of KRAS protein structure and dynamics. *Comput. Struct. Biotechnol. J.*, 18, 189–198.
37. Yamamoto, E. et al. (2012) Molecular dissection of premalignant colorectal lesions reveals early onset of the CpG island methylator phenotype. *Am. J. Pathol.*, 181, 1847–1861.
38. Sugai, T. et al. (2006) Analysis of molecular alterations in left- and right-sided colorectal carcinomas reveals distinct pathways of carcinogenesis: proposal for new molecular profile of colorectal carcinomas. *J. Mol. Diagn.*, 8, 193–201.